

# Crack (Non)Propagation in Amorphous Media

Tsviki Y. Hirsh and David A. Kessler

*Department of Physics, Bar-Ilan University, Ramat-Gan IL52900 Israel*

(Dated: September 23, 2004)

We study Mode I crack propagation in amorphous material via a molecular dynamics simulation of a binary alloy with pairwise central-force interactions. We find that when the system is subjected to constant displacement after introduction of a seed crack, the crack does not propagate. This was found to be true both for the modified Lennard-Jones potential of Falk and a shorter-range potential of our own devising. Crystalline samples prepared with these potentials exhibit normal brittle fracture, with running cracks. Only when subjected to a constantly increasing strain did the crack in the glasses lengthen. Even here, once the strain stopped increasing, the crack tip stopped moving. We examined the stress-strain curve for our model materials, and found that they did not exhibit the saturated stress plateau characteristic of ductile materials. We attribute the failure of crack propagation in this system to the availability of many meta-stable configurations available to the crack tip which serve to soak up the energy which would otherwise drive the crack. We conclude that this class of models is inadequate to describe crack propagation in brittle glasses.

## I. INTRODUCTION

The mechanism of crack propagation in amorphous materials, such as glasses, is still far from understood. There is good reason to believe that it exhibits significantly differences from fracture in crystalline solids. The first difference is the existence of a velocity gap, which is a necessary feature of a crystalline lattice system, but which has not been seen in experiments on amorphous systems. The second is the behavior of high velocity cracks. In crystalline lattices, above a certain velocity a Mode I crack no longer propagates along the midline. Rather, it chooses to bifurcate, and go off along some other easy propagation direction. This behavior has been seen both in experiments on crystalline silicon and in simulations of two-dimension crystals. Amorphous materials have no easy directions, and must do something different. Typically, they exhibit a form of "side-branching" behavior, in which daughter cracks are emitted which extend for some short distance, while the main crack keeps on propagating. A better theoretical grasp of fracture in amorphous materials is clearly desirable, in order to better characterize the novel features that such dynamics exhibits.

Surprisingly, there have been relatively few simulation studies of crack propagation in glasses, given that the vast majority of experiments have been performed using various brittle amorphous materials, with only a small number employing crystalline solids. This is no doubt at least in part a reflection of the increased technical difficulties in simulating glasses. Even constructing a simulation sample of glass without external stresses requires a delicate process of cooling, whereas an unstressed crystalline material is trivial to construct. A more subtle difficulty is connected to the nature of the length scales involved. Due to the singular nature of the continuum stress field around a crack tip, the fracture mechanism is exquisitely sensitive to the dynamics of bond-breaking at the atomic scale. In a crystal, this is the only scale, apart from the sample size itself, and thus it is relatively

easy to achieve essentially macroscopic results on systems only a few tens of lattice lengths wide. The microscopic structure of glasses is much more involved, with intermediate length scales that must also be resolved in order to achieve reliable results.

When surveying the existing simulation attempts to study crack propagation in glasses, one is immediately struck by the paucity of results, compared with the corresponding situation in crystalline systems. There has been, to our knowledge, no result that reproduces the basic experimental setup, namely a material with a seed crack that is subjected to a fixed external displacement, and then slightly perturbed so as to start the crack running the length of the system. Our basic point in this paper is that this situation is due to the fact that, for the class of models of glasses that have been examined to date, cracks *do not propagate*. The cracks that have been generated have been a result of systems which have been continually *pulled apart*, and not due to intrinsic crack propagation of the sort that has been seen in experiment, as well as in simulations of crystalline materials. The ductile/brittle transition which has been discussed in the literature<sup>1</sup> does not capture the distinction between freely running cracks and cracks which exist only due to continual pulling, which is the relevant one for crack propagation studies.

In this paper, we will first describe our model and simulation methods. In Section III, we will describe the stress-strain relationship we measure, and its implications. In Section IV, we will examine the behavior of a crack in our system.

## II. MODEL AND SAMPLE PREPARATION

The basic simulation framework we employ in this work is a 2D Molecular-Dynamics (MD) simulation, with a 2-body central force interaction between particles. We use the standard technique of mixing two sizes of particles in order to avoid crystallization. Binary alloy systems of

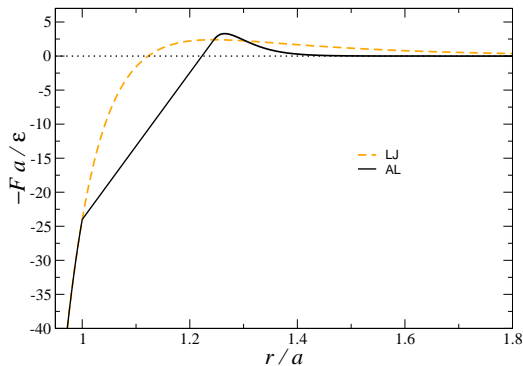


FIG. 1: The AL force law, compared to the standard LJ force

this type are known to exhibit a glass-transition when cooled from an initial high-temperature liquid state. This model is considered a good model for metallic glasses. Such metallic glasses exhibit very plastic and ductile behavior, in contrast to the very brittle glass that is used for fracture experiments. Such behavior was also seen by Falk and Langer<sup>2</sup> in his simulations of the stress-strain curve for a binary alloy Lennard-Jones (LJ) glass. Imposing a strain linearly increasing with time, Falk and Langer found that after an initial linear elastic regime, the stress saturated at some finite value. In other words, instead of breaking, the material began to undergo plastic flow. Clearly such a model is unsuitable for studying brittle fracture. To overcome this problem, Falk<sup>1</sup> introduced a modified interaction potential, which he termed a compressed Lennard-Jones (CLJ) potential. This CLJ potential had a narrower potential well, as well as a faster falloff at large distance as compared to the standard LJ potential. Falk found that with this new CLJ potential, the stress-strain relationship changed character, and now fell off beyond a critical strain. This is typically taken to be an indication of brittle behavior. As we shall see, the CLJ model nevertheless does not exhibit brittle fracture. To see to what extent this is generally true, we have employed in our simulations both the CLJ potential as well as a second potential which we introduce here. This new potential was designed to be even more brittle than the CLJ potential. Nevertheless, we found the qualitative fracture dynamics of the two potentials to be identical.

To understand why the LJ potential generates such a ductile material, let us consider the force law of the LJ potential :

$$f_{LJ}(r) = 48 \frac{\varepsilon_{ij}}{\sigma_{ij}} \left[ \left( \frac{\sigma_{ij}}{r_{ij}} \right)^{13} - \frac{1}{2} \left( \frac{\sigma_{ij}}{r_{ij}} \right)^7 \right] \hat{r}_{ij}, \quad (1)$$

After the force maximum at  $a_m \equiv (2 \cdot 2^{\frac{1}{6}} - 1) \cdot a$ , there is a very long attractive tail. This character of the LJ force law makes it very suitable for simulations of solidification. In order to have a force law that generates a brittle material, we have to shorten the attractive

TABLE I: Interaction parameters for binary mixture

$\varepsilon$	$\sigma$	
0.5	1	AA
0.75	0.8	AB
0.25	0.88	BB

tail. so that the material breaks almost immediately after a critical strain is applied. The ideally brittle force law is a "Piece-Wise Linear Force Law" namely a force law that shows a linear increase of force with increasing strain until a critical strain, and a zero force afterwards break down. This force law is the idealization of brittle behavior. However we cannot allow a too short tail, because it makes the glass solidification process very difficult. Therefore, we introduce a force law, which for convenient reference we call the AL (Almost Linear) force law, which is basically composed of a polynomial repulsive tail, as in LJ, a linear force for small deformations from equilibrium and an exponential decay of the force after the maximum force. In detail

$$f_{AL}(r) = \begin{cases} 48 \frac{\varepsilon_{ij}}{\sigma_{ij}} \left[ \left( \frac{\sigma_{ij}}{r} \right)^{13} - \frac{1}{2} \left( \frac{\sigma_{ij}}{r} \right)^7 \right] & r < a \\ \varepsilon_{ij} A + \varepsilon_{ij} B \cdot r & a < r < a_m \\ \varepsilon_{ij} C [1 + D(r - a_m)] e^{-\beta(r - a_m)} & r > a_m \end{cases} \quad (2)$$

Where A,B,C,D depend on  $\sigma_{ij}$  and are chosen so as to make the force continuous, and  $a_m = (2 \cdot 2^{\frac{1}{6}} - 1) \cdot a$  is the location of the LJ maximum force. The effective radius which corresponds to the potential minimum is  $a_0 = 1.222a$  and the potential well depth is  $\varepsilon_0 = 2.66\varepsilon$ . For computational efficiency, we compute the force via a cubic-spline interpolation, which ensures that the derivative of the force is continuous.

Our system consists of a binary mixture of particles, 80% large particles (A-type) and 20% small particles (B-type). Both types of particles have the same mass (set to be 1), and different force parameters, as indicated in Table 1.

The parameters were chosen in order to achieve interaction properties similar to the LJ potential<sup>3</sup>. Several other sets of parameters are employed in literature, designed to model various specific glasses. However our interest is the fracture process and not in modeling some particular real glass, and so any set of parameters which generates a glassy material is sufficient for our purposes. The MD simulations were performed using a half step leap-frog algorithm, with a time step of  $\Delta t = 0.001$ . We start by randomly placing particles (A or B) on the simulation square, in the form of a square lattice. Periodic boundary conditions were applied, so that the whole process is done via constant density. The density is taken to be a bit larger than necessary, in order to avoid creation of holes inside the glass.

We let the system to mix while holding the temperature in a very high value of  $5.1 \frac{\epsilon_0}{k_B}$  throughout 20,000 time steps. The system temperature is controlled by scaling of the particles velocities once every few time steps, according to the desired temperature<sup>4</sup>.

After the system is mixed, we gradually reduce the temperature across the system by a temperature decrease rate of  $10^{-6} \frac{deg}{timestep}$ , to a temperature level of  $4.5 \frac{\epsilon_0}{k_B}$ . we let the system to relax by holding the temperature on a constant value for 10,000 time steps. The process continues by gradually reducing the temperature to lower temperature levels (3.5, 2.5, 2, 1.8 ...), while in every temperature level we hold the temperature constant for 10,000 time steps.

This model is known to pass through a glass transition at about  $0.3 \frac{\epsilon_0}{k_B}$ ; afterwards the particles configuration stays approximately fixed. After the system reaches a temperature of  $0.05 \frac{\epsilon_0}{k_B}$ , well under the glass transition, a small Kelvin type friction<sup>5</sup>,  $f_{ij}^K = \eta(v_i - v_j)$ , with  $\eta = 0.08$ , is turned on in order to reduce the temperature to zero. This process takes approximately another 100,000 time steps. After the glass has been fully relaxed, we cut its edges from the periodic boundary conditions, and again allow it to relax slowly to adjust to the change of pressure, giving us finally our rectangular piece of glass.

Strain is imposed on our sample by displacing the last few rows of particles near the top and bottom edges to be displaced according to the desired strain, and freezing any subsequent motion. To impose an initial seed crack, we solved for the continuum elastic solution of a seed crack of a given length in a rectangle of the same aspect ratio as our sample. This calculation was performed using a multigrid technique described in Ref. 6,7. We then interpolated this solution to the equilibrium locations of the particles in our sample, and gave the particles the corresponding displacement. We then relaxed our sample for some time to allow it to return to equilibrium.

### III. CRACKS

To study the dynamics of cracks in our system, the natural experiment to perform is to seed an initial crack with some given external displacement, to perturb the crack tip and analyze the crack motion. This is exactly the experimental protocol used in the Fineberg experiments. However, when we attempted this using the CLJ potential, the crack refused to run. No matter how large the initial perturbation, or its precise form, the crack would almost instantly stop, with a reorganization of the particles in the vicinity of the crack tip.

To see if perhaps the potential was not "brittle" enough, we repeated the experiment using our new potential. Again the crack tip refused to run. As a test, we created a crystal with our new potential, and repeated the experiment. Now the crack had no problems running, producing results very similar to what is seen in lattice simulations.

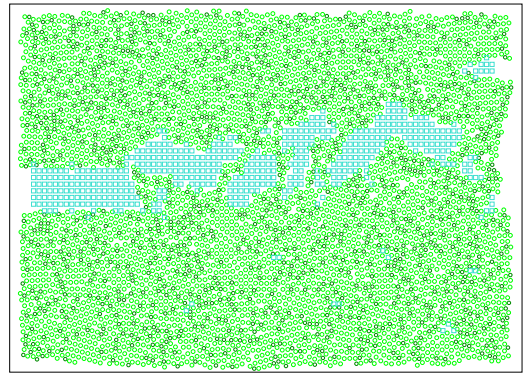


FIG. 2: Configuration of particles at end of run. Strain rate= $\times$ . System size was  $\times$ .

Given that Falk had produced "running" cracks with the CLJ potential, the difference must be attributed to the different experimental protocol. In Falk's work, instead of using a constant external displacement, he employed a displacement growing linearly in time. We then repeated our simulation, this time like Falk using a displacement increasing linearly in time. This did indeed produce "running" cracks. (See Fig. 2 for a picture of the crack at the end of the run.) Clearly then, the strain rate is an important parameter. We ran simulations for a range of strain rates, producing the results in Fig. 3a. The crack length indicated in the Figure was determined by partitioning the sample into squares of size a lattice spacing, and counting the number of squares not containing particles. In this count, empty squares not touching another empty square were ignored, so as not to include isolated voids in the measurement. If instead of plotting crack length as a function of time, one plots it versus the instantaneous external displacement, one sees in Fig. 3b that all the curves collapse. Thus the crack length is a function of the external displacement only. This is in complete contrast to the standard dynamical fracture scenario, where the external displacement is *constant* in time, and the crack length increases nonetheless, due to its own internal dynamics. In these model glasses, however, the crack dynamics is for some reason completely damped, and the crack responds only to continually increasing external driving.

A striking way to verify this diagnosis is to turn off the strain increase in the middle of the run. The results of this are presented in Fig. 4. We see that as soon as the strain increase is turned off, with the strain remaining constant afterwards, the crack stops dead in its tracks. This is despite the fact that the crack is propagating at a significant velocity prior to the turning off of the strain increase.

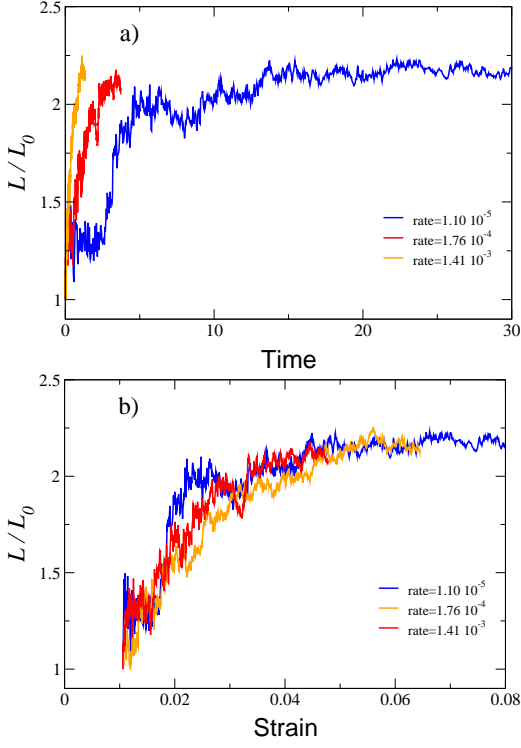


FIG. 3: a) Crack length versus time for three different strain rates. b) Same data plotted as a function of strain. The samples consisted of 6000 particles with an aspect ratio of 1.6. The length  $L_0$  of the initial seed crack was  $1/5$  of the length of the sample.

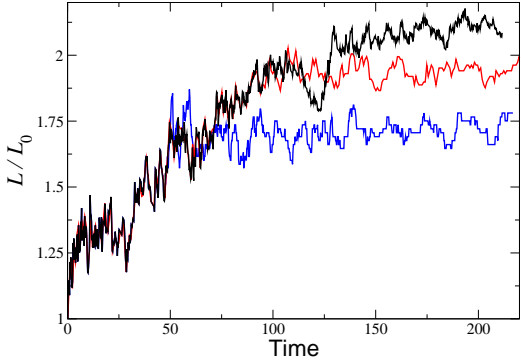


FIG. 4: Crack length versus time. The top curve is the same data as in Fig. 3. The lower curves portray simulations where the strain increase was turned off at various times. The immediate cessation of further fracture is evident.

#### IV. STRESS-STRAIN RELATIONSHIP AND INTERNAL DAMPING

We saw in the previous section that our model glasses did not support running cracks. Thus must therefore possess some sort of internal damping mechanism that is capable of soaking up the energy associated with the stress release of the bulk as the crack lengthens. In order to understand this better, we turn to a closer examina-

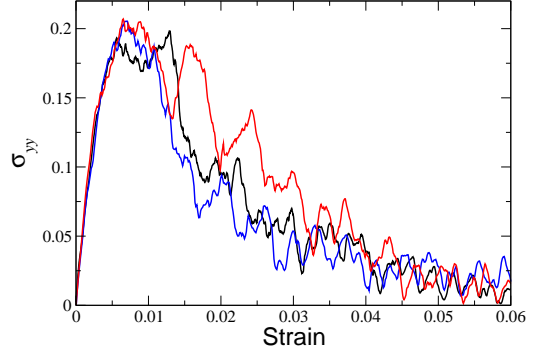


FIG. 5: Stress-Strain curves for three different samples of the same AL glass. Strain rate was  $1.76 \cdot 10^{-4}$ . Samples were 6000  $\mu$

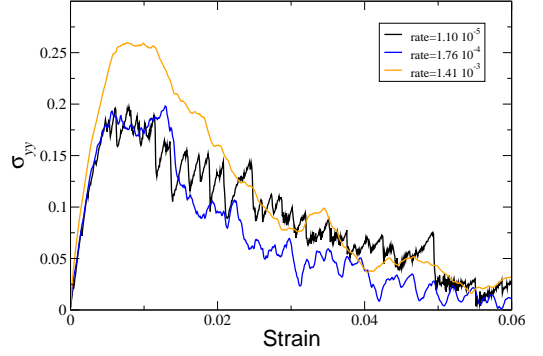


FIG. 6: Stress-strain curves for three different strain rates. The sample was as in Fig. 5.

tion of the stress-strain relationship. The stress tensor element -  $\sigma_{yy}$  is measured, as we increase the strain  $-\varepsilon_{yy}$  from zero, with a slow strain rate. The strains increased linearly with time,  $\Delta = b \cdot t$ , where  $b$  is the strain rate (dimensions of  $[\frac{1}{time}]$ ). The stress tensor is measured by using the virial expression<sup>4</sup>.

$$\sigma_{\alpha\beta} = \frac{NT_{\alpha\beta}}{V} + \frac{1}{2} \sum_{i < j}^N r_{ij}^{\alpha} \cdot f_{ij}^{\beta} \quad (3)$$

Where  $\alpha, \beta \in xy$ ,  $i, j \in 1 \dots N$ ,  $N$  is the number of particles,  $V$  is the system volume and  $T_{\alpha\beta} = \frac{1}{N} \sum_i v_i^{\alpha} v_i^{\beta}$  indicates the system temperature.

Figure 5 shows stress-strain curves for 3 different realizations of a glass formed using our AL force law. Each simulation uses 6000 particles and a strain rate of  $1.76 \cdot 10^{-4}$ . In the region of small strains, the material shows an elastic behavior, with reversible deformation. This is the region of the graph which shows a linear dependence of the stress with strain. At  $\Delta \sim 0.1$  a first break down occurs as the stress drops to lower values. Note that the drop of stress is not one sudden and continuous break, as expected from a brittle material, but rather composed of a series of small sharp drops. Each small stress drop corresponds to opening of voids in the

glass, which reduce the stress across the system. Between the elastic zone and breakdown there is a narrow area of plastic flow, namely more or less constant stress, while the strain increases. This area of the graph corresponds to opening of very small holes all over the glass. However, this region is narrow, in contrast to very long plastic flow regions that other studies have found, using LJ<sup>2</sup> and Stillinger-Weber<sup>8</sup> laws. In this respect, the AL force law is qualitatively similar to the CLJ force of Falk. We see also that while different in detail, the overall features of the curves for the three samples are the same. Also, the bulk linear elastic properties at small strain are nearly identical, as one would expect. Measurements on larger systems also produced very similar results.

Even though our AL force law exhibits breakdown, with only a restricted plastic flow regime, its behavior cannot be characterized as truly brittle. In an ideal brittle material, the stress would quickly fall to zero after the yield stress is reached. Here however, the stress does not fall to zero, even for strains a few times critical. More importantly, the fall is not smooth and consists of many spikes. This indicates the existence of many energy barriers encountered in the fracture process. This spikiness was studied in great detail by Gagnon, Patton and Lacks (GPL)<sup>8</sup> (albeit in a region of plastic flow). They showed that the origin of this phenomenon was in the ability of the material to locally reconfigure itself into a new metastable state. We believe that this is at the heart of the inability of our model material to support running cracks. The material can soak up the elastic energy by continually finding new local metastable configurations of the crack tip region. These metastable configurations do not exist in a crystalline material. This would explain why a crystal formed using the same force-law is able to support running cracks.

It is also instructive to consider the stress-strain curve for different rates of strain increase. This is presented in Fig. 6. We see that the general trend is that at the higher strain rates, the fall of the stress is smoother, with

fewer and smaller spikes than seen at low strain rate. It would appear that there is a time scale associated with the construction of a new metastable configuration. If the strain rate is too high, the system does not have time to find this new state. We also verified that if the strain increase was halted, further cracking ceased essentially immediately.

## V. DISCUSSION

In this work, we have seen that the model glasses we have considered do not support running cracks. This is despite the fact that the stress-strain curve for these materials exhibits only a very small plateau which would be indicative of ductile behavior. The question that remains is how to achieve brittle fracture behavior in a model of glass. Clearly some model must work, since experimental brittle glasses are common. We are faced with a situation where traditional measures insufficiently characterize the dynamical fracture behavior of a material. A similar situation was encountered with the standard Stillinger-Weber model of crystalline Si, which was found to be not brittle<sup>9</sup>, in contradiction to the experimental situation. A related issue is what aspect of the model is responsible for the existence/nonexistence of running cracks. Our guess is that it is related to the degree of crystalline order. It seems possible to us that if a model exhibits sufficient short-range order, it should exhibit running cracks. This is related to the question of time-scales discussed above in the context of the stress-strain curve. If the crack is moving quickly enough on the time-scale necessary to find a new metastable tip configuration, then the crack will continue to run. It is reasonable to suppose that the stronger the short-range order, the longer this reorganizational time-scale will be. We hope to test these ideas in a future work.

---

<sup>1</sup> M. L. Falk, Phys. Rev. B **60**, 7062 (1999).

<sup>2</sup> M. L. Falk, J. S. Langer, Phys. Rev. E **57**, 7192 (1998).

<sup>3</sup> W. Kob and H. C. Andersen, Phys. Rev. E **51**, 4626 (1995).

<sup>4</sup> D. C. Rapaport, *The Art of Molecular Dynamics Simulation* (Cambridge University Press, Cambridge, 1995).

<sup>5</sup> D. A. Kessler and H. Levine, Phys. Rev. E **63**, 016118 (2001).

<sup>6</sup> D. A. Kessler and H. Levine, Phys. Rev. E **68**, 036118 (2003).

<sup>7</sup> E. Bouchbinder, D. A. Kessler, and I. Procaccia, "Velocity Fluctuations in Dynamical Fracture: The Role of Microcracks", preprint, cond-mat/0403680 (2004).

<sup>8</sup> G. Gagnon, J. Patton, and D. J. Lacks, Phys. Rev. E **64**, 051508 (2001).

<sup>9</sup> J. A. Hauch, D. Holland, M. P. Marder, and H. L. Swinney, Phys. Rev. Lett. **82**, 3823 (1999).